Characterising flow within a manhole under two surcharge heights using Particle Image Velocimetry

J. Nawasra[1], S. Lau[2], V. Stovin[2], I. Guymer[1], P. Dunkley[1], P.J. Bryanston-Cross[1]

[1]*Division of Civil and Mechanical Engineering, School of Engineering, University of Warwick, Coventry, CV4 7AL, UK. (email j.nawasra@warwick.ac.uk)*
[2]*Department of Civil and Structural Engineering, University of Sheffield, Sheffield, S1 3JD, UK.*

Introduction

The efficient design and management of urban drainage systems with respect to water quality processes requires knowledge of solute retention times. Within uniform conduits, these may be estimated using the discharge and cross-sectional shape. However, within urban drainage structures – such as manholes, storage tanks and separators – estimation of solute travel time is less straightforward. This is especially so under high flow conditions when the system becomes surcharged. Recent laboratory and field studies quantifying retention times within urban drainage structures have employed tracing techniques to measure and analyse changes in temporal concentration distributions across the structures (Shepherd *et al.*, 2001 and Guymer *et al.*, 2002).

Manholes occur commonly within urban drainage systems wherever changes in flow direction, pipe slope, diameter or elevation are required. During normal dry weather flow in a combined sewer system the pipes are designed to flow partially full. However, under storm conditions the pipes and manhole structures may become surcharged. Observations of the movement of a passive tracer within a surcharged model manhole have provided a qualitative description of the flow field. Guymer *et al.* (2005) identified an interesting solute transport characteristic under surcharged flow condition, and this has also been observed in a scale manhole model (Lau *et al.*, in press). The model results revealed a sharp transition in the median travel time as shown in figure 1a. At surcharge depths below the threshold level where the transition occurred, the travel time showed a linear relationship with surcharge ratio, whilst above the threshold surcharge level, the travel time dropped to a low and constant level. The typical temporal concentration distributions observed at high and low surcharge, shown in figure 1b, suggest that at low surcharge depths, solutes experience instantaneous mixing within the stored volume, whilst at high surcharges depths, a large proportion of the tracer is advected through the manhole, experiencing little mixing. The same laboratory configuration has been used for the study reported here.

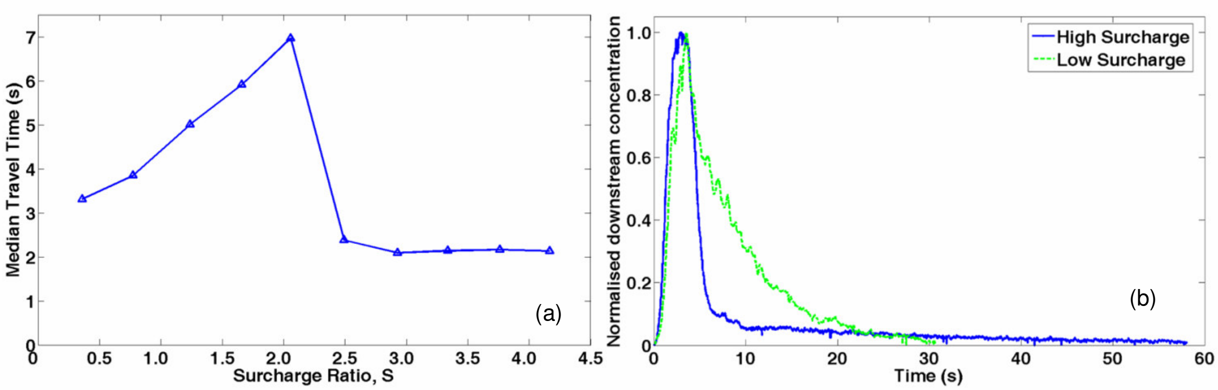

Figure 1a – Relationship between travel time and surcharge ratio for the 218 mm diameter manhole at 0.35 l/s
Figure 1b – Effects of high and low surcharge on downstream temporal concentrations

The aim of this work was to characterise the flow field within a surcharged manhole under two contrasting hydraulic conditions using Particle Image Velocimetry (PIV). PIV allows accurate, quantitative measurements of fluid velocity at a large number of points in a plane simultaneously. The technique uses a planar light sheet for illumination and a recording device, such as a CMOS camera, positioned orthogonal to the plane of illumination, to record the movement of seeding particles in a planar region of interest. Fluid velocities are quantified based on the displacement of the seeding particles. The technique has gained popularity over the last 20 years and has become a well established experimental technique in fluid dynamics research (Adrian, 2005).

Laboratory Set-up

A transparent Perspex model of a manhole was used to obtain optical access to the main chamber. Surcharge depths of 78 mm and 28 mm were considered, with a constant flow rate of 0.35 l/s. Two horizontal and three vertical planes were analysed for both surcharge conditions to provide comprehensive and quantitative insights into the three-dimensional flow field. The manhole model (Lau *et al.*, in press) has a main circular chamber with an internal diameter of 218 mm, with diametrically opposite inlet and outlet pipes of 24 mm internal diameter at the base shown in figure 2a. Note that surcharge depth is defined with respect to the soffit of the inlet pipe.

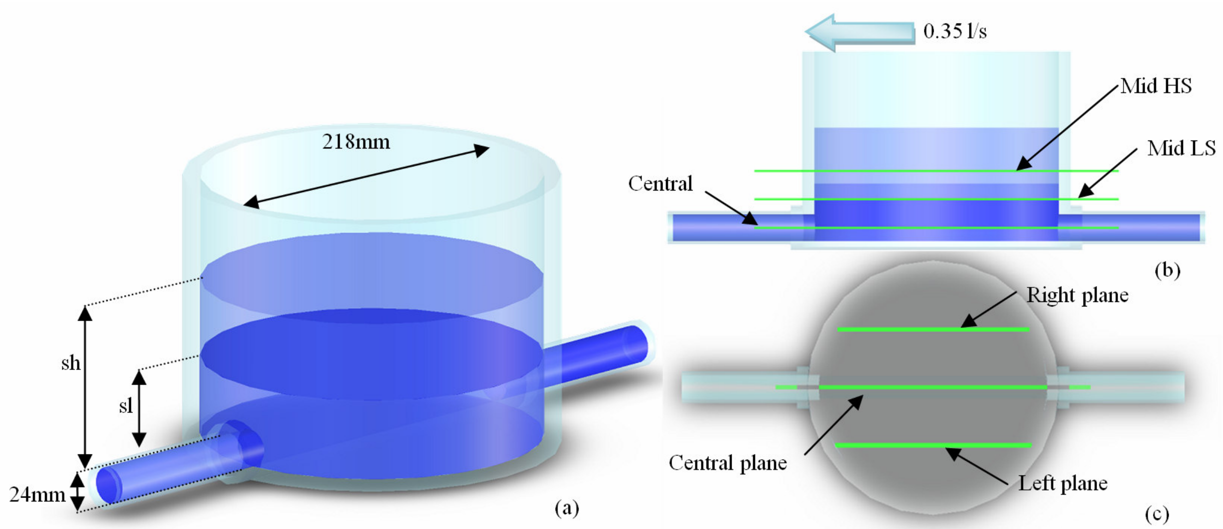

Figure 2a – Water levels in the high (sh = 78 mm) and low (sl = 28 mm) surcharged manhole
Figure 2b – Horizontal light sheet position (side view)
Figure 2c –Vertical light sheet position (plan view)

The position of the horizontal light sheets is shown in figure 2b. The central horizontal plane is positioned on the centreline of the inlet and outlet pipes. The 'Mid HS' and 'Mid LS' planes are positioned equidistant from the pipe soffit and the free surface. The placement of the vertical light sheets is shown in figure 2c. The central vertical plane is positioned on the centre line of the inlet and outlet pipe. The left and right planes are midway between the central plane and the circumference of the main chamber.

A 5 Watt continuous wave Argon-ion laser (λ = 514 nm), coupled with a rotating octagonal mirror and a parabolic mirror, were used to produce a scanning light sheet of the order of 2mm in thickness and with variable scanning frequency. A Photron PCI-1024 high speed camera operating at 500 frames per second with a spatial resolution of 1024 x 1024 pixels x 8 bits was used to capture the illuminated particles in the flow. The flow was seeded with neutrally buoyant Polyamide particles (mean diameter 50 µm; density 1.03 kg/m^3). The seeding particles scatter the laser light towards the camera and provide excellent contrast with the background, ensuring reliable correlations during data processing. Figure 3a and 3b show examples of the images acquired for a vertical and a horizontal plane respectively. It is important to note that the frequency of the scanning light sheet was matched to the framing rate of the camera to ensure a single exposure of every particle was captured. This eliminates multiple exposures and reduces the likelihood of particle streaking which may result in inaccuracy when approximating particle centres in subsequent PIV analysis.

The camera buffer stores 4GB of data, which equates to 3200 time series images, providing 6.4 seconds of data per run. Three repeat runs were performed for each test case to provide 18.2 seconds and 9600 frames. This also provided data in order to evaluate the repeatability of the experimental runs. Each pair of frames provides a single time-resolved instantaneous vector map, which allows fundamental parameters of the mean velocity such as turbulence intensity, turbulence kinetic energy and Reynolds stresses to be calculated with high temporal resolution. This data may be useful for comparison with future CFD predictions. The data analysis was performed using LaVision's flow analysis software, DaVis. The data required minimal pre-processing; a mask was applied to enforce the physical boundary of the tank walls to remove erroneous vectors outside the region of interest and to reduce computational time.

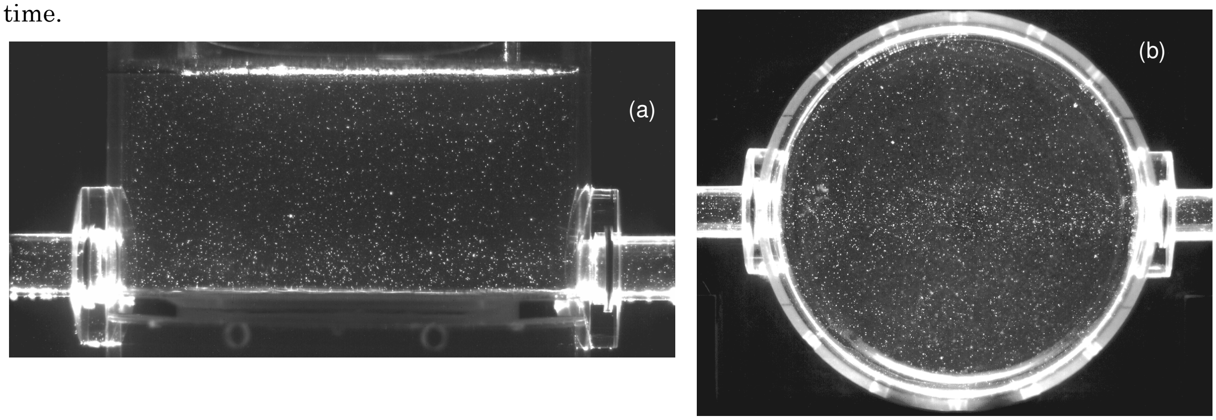

Figure 3 – Example raw images acquired by the high speed camera, (a) a vertical plane (b) a horizontal plane

A cross correlation technique was employed as the scattered light from the particles was recorded as a single exposure over consecutive frames. All adjacent pairs of images were cross correlated. The vector processing subdivides the image into interrogation windows and each window is evaluated by cross-correlation. A vector is calculated for every window. A multi-pass decreasing tile size cross-correlation was employed to calculate the vector fields. A large window size was chosen in the first pass to capture the large scale fluid displacement, whilst a smaller tile size in the second pass ensured the smaller scale motion was also resolved. This provided a reliable vector map which includes the entire range of flow structures. The options chosen for the window sizes in the multi-pass process vary slightly depending on the data set, but typically a 32 x 32 maximum window size with a 50% overlap, reducing to 12 x 12 pixel window overlapped by 25%. These are typical settings for a flow showing a maximum pixel displacement of between 8 and 15 pixels. Time averaged velocity vectors for each of the five, two dimensional measurement planes are presented to illustrate the dominant flow features within the highly three dimensional flow. The time averaged data is plotted with the coloured contours representing the in-plane velocity magnitude and the superimposed vector field showing the direction of the fluid motion.

Results & Discussion

The results reveal significant difference between the flow regimes across the two surcharge conditions, reinforcing the conclusions drawn from figures 1a and 1b. Figure 4 compares the differences between similar planes at the two surcharge heights. The horizontal central plane is representative of the difference observed across all horizontal planes. A noticeable symmetry occurs in the horizontal central plane in figure 4a. The high velocity fluid enters the main chamber as a jet, forming a coherent stream towards the exit. Two symmetrical return currents occur either side of the outlet, with recirculating flow in both sides of the chamber moving back towards the inlet. The low surcharge case in figure 4b does not exhibit the symmetry shown in the high surcharge case. The direction of jet skew is sometimes reversed in repeat experiments. The asymmetric jet appeared to experience a low frequency fluctuation, although the timing and spatial extent of the fluctuation has not been comprehensively identified due to the comparatively short duration of the PIV measurement.

Figure 4c shows a clear vertical recirculation in the high surcharge case. This is expected to cause water to remain within the upper surcharge volume for an extended period of time, whilst the dominant jet enters and exits at high speed, thereby short-circuiting the main storage volume of the structure. Figure 4d shows the low surcharge vertical central plane and the coherent jet observed in figure 4c is no longer recognisable. The shear layer of the jet appears to interact directly with the free surface, efficiently mixing the incoming fluid with the fluid in the main chamber.

A convenient way to verify the consistency of the data obtained from the horizontal and vertical planes is to plot the x-velocity on the line of intersection between the two planes. Figure 4e and 4f show x-velocities on the line of intersection for the high and low surcharge respectively. The figures show very good similarity between the two profiles, which confirms the high level of consistency between the data sets. Small deviations are visible in the low surcharge plots as the low frequency skewed jet makes minor positional changes.

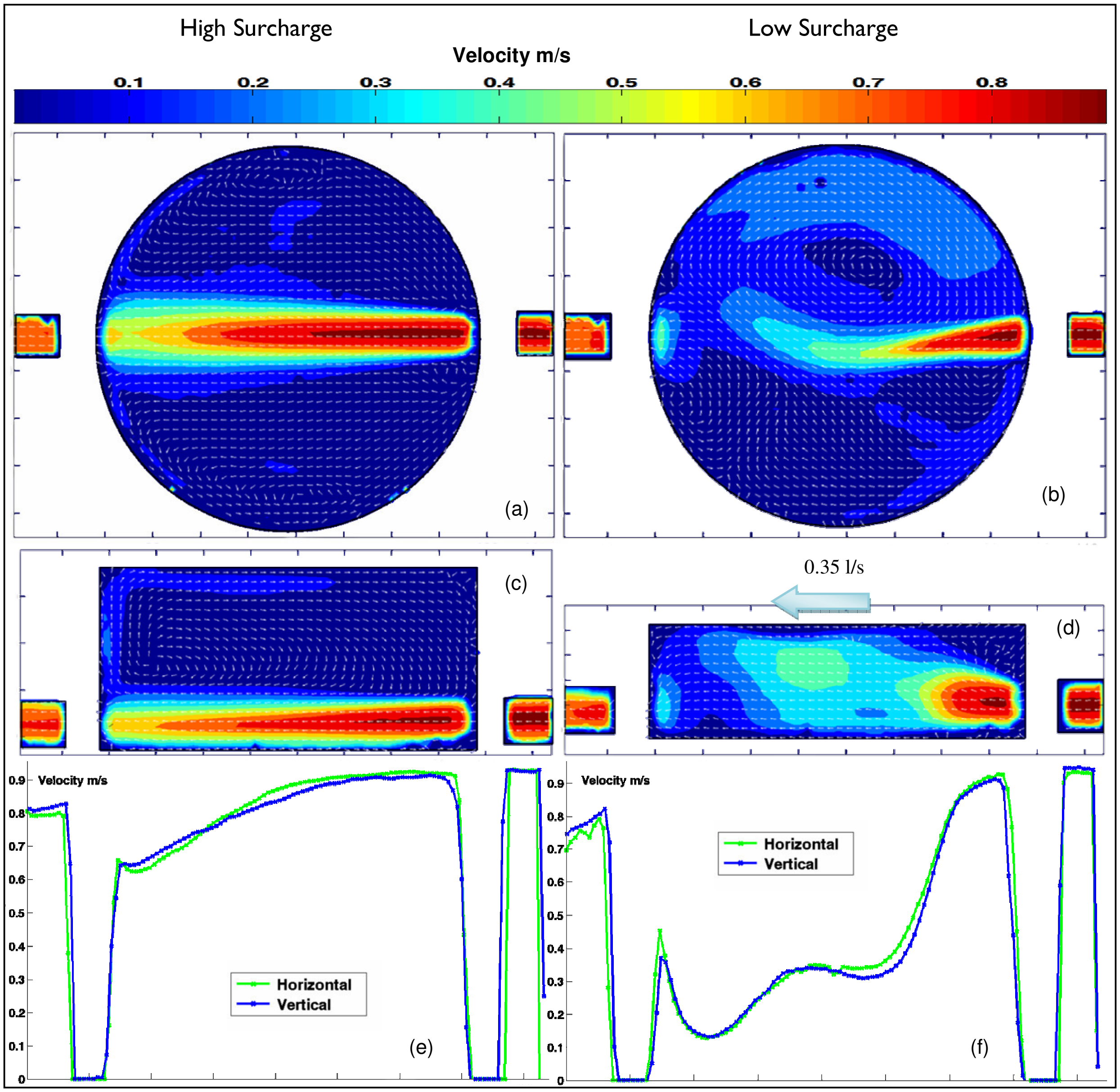

Figure 4 – Comparison of high and low surcharge time averaged velocity across the central planes a & b – Horizontal central plane, c & d – Vertical central plane e & f – x-velocities on the line of intersection between the horizontal and vertical planes

In the region of the inlet and outlet it may be seen that the velocity apparently drops to zero. This is clearly erroneous, and is attributable to the spatial averaging processes inherent in DaVis's adaptive multi-pass algorithm, in combination with tile size and mask positioning options. This limitation means that data corresponding to a zone approximately 10 mm wide inside the manhole from both the inlet and outlet requires further analysis to remove these effects.

A high degree of symmetry occurs in the left and right vertical planes, shown in figure 5a and 5c for the high surcharge case. The contour and vector plots show almost identical flow fields with a dominant clockwise recirculation. The low surcharge case shown in figures 5b and 5d does not exhibit the single vertical recirculation. Instead the plane can be divided into two regions. The left plane reveals a recirculation in one half and a dominant single uni-direction flow in the general direction of the outlet. In the right plane the recirculation occurs higher up and the uni-direction flow is in the opposite direction to the left plane. The higher velocities shown in the right plane are almost certainly linked to the position of the skewed jet. This is another example of the consistency shown between separate planes of data within this study.

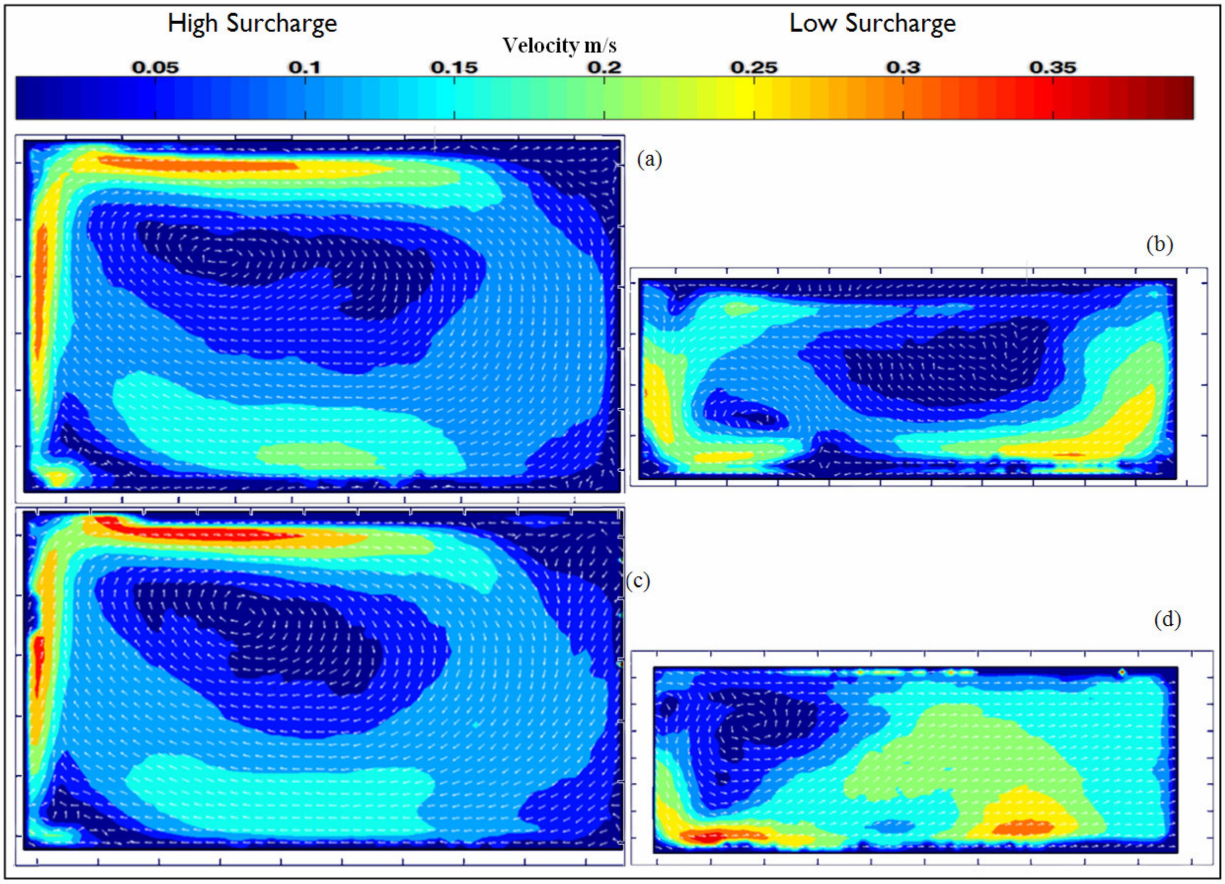

Figure 5 - Comparison of high and low surcharge time averaged velocity across left and right planes
a & b – Left vertical planes, c & d – Right vertical planes

The mid surcharge depth horizontal plane is shown in figure 6. The high surcharge case shows some deviation away from a purely symmetrical pattern. The bulk of the flow in this region is out of plane, so the velocities recorded in this plane are much lower than in any other plane. In contrast, the low surcharge mid surcharge depth plane in figure 6b indicates velocities comparable with the horizontal central plane. These two planes are closer together and are more likely to show similar features. The skewed jet is captured again in this plane with a major re-circulation in the right hand side of the chamber and three smaller re-circulations in the left side.

The turbulent kinetic energy (V_{tke}) is calculated using equation 1, by first finding the root mean square (V_{rms}) of the velocity using equation 2 (DaVis Manual) and displayed in figure 6c and 6d.

$$V_{tke} = |V_{rms}|^2 \qquad \text{Eq.1}$$

$$V_{rms} = \sqrt{\frac{1}{(n-1)} \sum_{i=1}^{n} (V_i - V_{avg})^2} \qquad \text{Eq.2}$$

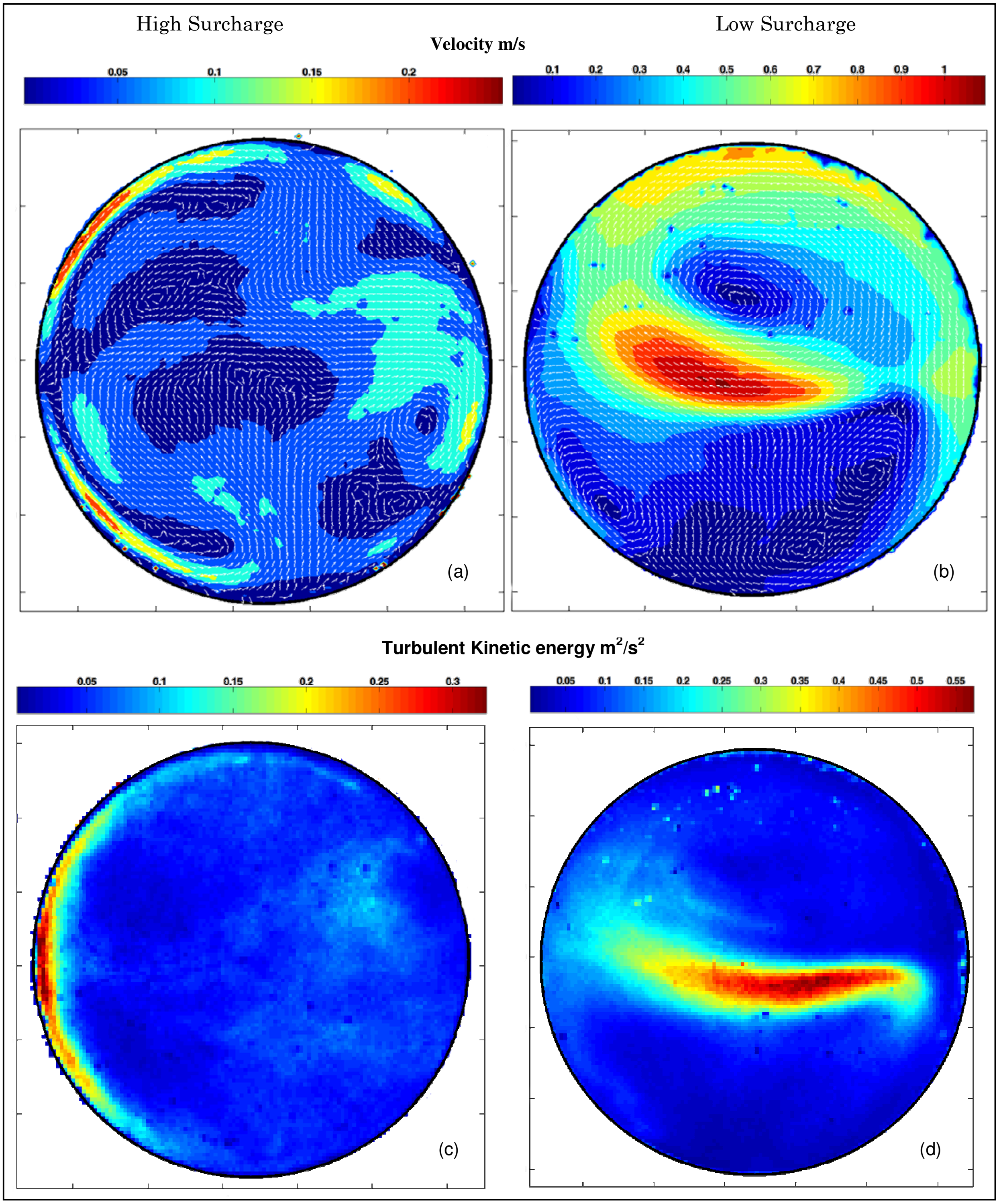

Figure 6 - Comparison of the mid surcharge depth planes
a & b – Time averaged velocity, c & d – Turbulent kinetic energy

The difference in turbulent kinetic energy between the two surcharge cases is highlighted, with the low surcharge showing approximately 2 times the turbulent kinetic energy of the high surcharge case.

The accuracy of the PIV measurements is estimated to be 5-15%. This has been determined by calculating and summing the errors associated with spatial discretisation, scaling, temporal inaccuracies and out of plane motion within light sheet.

Conclusions

- Five planes of PIV data have been measured, which help to describe the flow structures within a scale model of a manhole under high and low surcharge conditions.
- The high surcharge case exhibits high levels of symmetry in the horizontal and vertical direction with a clear coherent jet forming. Fluid travels straight through the system due to the presence of the high velocity jet and therefore does not mix effectively with the fluid in the manhole, yielding small mean travel times.
- The low surcharge case does not exhibit symmetry horizontally or vertically. The mean travel time within the low surcharge system is significantly higher, which is attributed to its more efficient mixing.
- The work serves to highlight the different flow regimes within the manhole, providing a better understanding of solute transport within urban drainage systems and will assist with the validation of CFD simulations and the derivation of generic, scalable, models for characterising dispersion in manholes.

References

Guymer, I., Dennis, P., O'Brien, R. and Saiyudthong, C. 'Diameter and Surcharge Effects on Solute Transport across Surcharged Manholes', A.S.C.E., Journal of Hydraulic Engineering, 2005, 131, 4, 312-321.

Guymer, I., Shepherd, W.J., Dearing, M., Dutton, R. and Saul, A.J. 'Solute Retention in Storage Tanks 9th Int. Conf. On Urban Drainage, 8th-13th Sept. 2002, Portland, USA, pp 1-11.

Lau, S.D., Stovin, V.R. and Guymer, I. 'The prediction of solute transport in surcharged manholes using CFD', *Water Science and Technology,* 55(4), 57-64, 2007.

Lau S. D., Stovin V. & Guymer I. (accepted in 2007). 'Scaling the Solute Transport Characteristics of Surcharged Manholes'. Urban Water.

Shepherd, W.J., Guymer, I. and Saul, A.J. 'Solute retention and mixing characteristics in CSO structures', A.S.C.E., World Water and Environmental Resources Congress, Urban Drainage Modelling Symp., May 20-24, 2001, Florida, USA.

Adrian, R.J. 'Twenty years of particle image Velocimetry', Experiments in Fluids, 2005, 39, p159-156

Davis 7.1 Software Manual for DaVis 7.1 by Lavison, July 2005